Nano-multilamellar lipid vesicles promote the induction of SARS-CoV-2 immune responses by a protein-based vaccine formulation

Monica Josiane Rodrigues-Jesus, PhD[a,f,1], Marianna Teixeira de Pinho Favaro, PhD[a,b,1],
Aléxia Adrianne Venceslau-Carvalho, MSc[a,b], Maria Fernanda de Castro-Amarante, PhD[a,b],
Bianca da Silva Almeida, PhD[e], Mariângela de Oliveira Silva, PhD[a,b,e],
Robert Andreata-Santos, PhD[c], Cecilia Gomes Barbosa, PhD[d], Samantha Carvalho Maia Brito[a],
Lucio H. Freitas-Junior, PhD[d], Silvia Beatriz Boscardin, PhD[e],
Luís Carlos de Souza Ferreira, PhD[a,b,*]

[a]Laboratory of Vaccine Development, Department of Microbiology, Institute of Biomedical Sciences, University of São Paulo, São Paulo, Brazil
[b]Scientific Platform Pasteur/USP, University of São Paulo, São Paulo, Brazil
[c]Retrovirology Laboratory, Immunology and Microbiology Department, Federal University of São Paulo, São Paulo, Brazil
[d]Phenotypic Screening Platform of the Institute of Biomedical Sciences of the University of São Paulo, São Paulo, Brazil
[e]Laboratory of Antigen Targeting for Dendritic Cells, Department of Microbiology, Institute of Biomedical Sciences, University of São Paulo, São Paulo, Brazil
[f]Division of Infectious Diseases and International Health, University of Virginia School of Medicine, Charlottesville, VA, USA

Revised 25 July 2022

Abstract

The development of safe and effective vaccine formulations against severe acute respiratory syndrome coronavirus 2 (SARS-CoV-2) represents a hallmark in the history of vaccines. Here we report a COVID-19 subunit vaccine based on a SARS-CoV-2 Spike protein receptor binding domain (RBD) incorporated into nano-multilamellar vesicles (NMV) associated with monophosphoryl lipid A (MPLA). The results based on immunization of C57BL/6 mice demonstrated that recombinant antigen incorporation into NMVs improved antibody and T-cell responses without inducing toxic effects under both in vitro and in vivo conditions. Administration of RBD-NMV-MPLA formulations modulated antigen avidity and IgG subclass responses, whereas MPLA incorporation improved the activation of $CD4^+/CD8^+$ T-cell responses. In addition, immunization with the complete vaccine formulation reduced the number of doses required to achieve enhanced serum virus-neutralizing antibody titers. Overall, this study highlights NMV/MPLA technology, displaying the performance improvement of subunit vaccines against SARS-CoV-2, as well as other infectious diseases.
© 2022 Elsevier Inc. All rights reserved.

Keywords: Nano-multilamellar vesicles; Lipid-based nanoparticles; Vaccine; SARS-CoV-2; RBD

Introduction

Severe acute respiratory syndrome coronavirus 2 (SARS-CoV-2) was first reported in Wuhan, China, in late 2019. The high transmissibility and associated rapid global spread of the virus resulted in a pandemic that may persist for several years [1]. Numerous mutations of the SARS-CoV-2 viral genome and the consequential emergence of exceedingly transmissible variants have resulted in an uncontrolled spread of the virus in several countries. Currently, approximately half a billion confirmed cases and six million deaths have been reported worldwide [2]. As such, the spread of SARS-CoV-2 is still regarded as a serious public health concern that necessitates integrated global efforts to develop effective preventive and therapeutic measures [3,4]. The prime and most successful example of this is the expeditious development of various coronavirus disease (COVID-19) vaccines and subsequent public accessibility thereof, representing an unparalleled hallmark in the history of vaccinology [5–11].

SARS-CoV-2 is an enveloped, single-stranded RNA virus that is 80–120 nm in diameter and consists of nearly 30,000 base pairs, encoding structural (S, E, M, and N) and non-structural proteins [12]. The spike (S) protein, located on the viral particle surface as a homotrimer, has been extensively researched, particularly as a target for vaccine development. The S protein contains the receptor-binding domain (RBD), a region responsible for virus binding to host cell receptors, such as the angiotensin-converting enzyme (ACE2), present in epithelial cells of the lungs, intestine, heart, and kidney [13].

The efficiency of recombinant protein utilization as antigen targets is reliant on the combined use of delivery systems and adjuvants [14]. Considering this, nanoparticles may improve the immunogenicity of antigens, owing to their physicochemical characteristics, intrinsic capability to target antigens to immune cells, and inherent adjuvant effects. For instance, lipid nanoparticles have been reported to protect antigens from degradation by plasma proteins, promote antigen delivery to cells involved in both innate and acquired immune response modulation, and mimic the virus surface by presenting the target antigens in a multivalent manner [15–21]. Nano-multilamellar vesicles (NMVs) represent a particular class of nanosized lipid vesicles previously used in vaccine studies with bacterial and viral-derived antigens [20,21]. Administration of antigen-loaded NMVs results in an enhanced immune response compared to that of vaccines containing only the purified protein combined with conventional adjuvants [20,21]. In addition, NMVs allow for the incorporation of antigens and immunostimulant molecules, such as FDA-approved monophosphoryl lipid A (MPLA), a non-toxic portion of bacterial lipopolysaccharide (LPS). MPLA exerts an immunostimulatory effect by activating innate immune cells, thereby stimulating antigen-presenting cells and, subsequently, effector T and B cells. Thus, antigen-specific adaptive immune responses, including immunological memory, may be mediated by MPLA [22–25].

In the current study, a novel vaccine formulation comprising a combination of recombinant SARS-CoV-2 RBD protein and MPLA in NMVs was evaluated. The results demonstrated that RBD-loaded NMVs boosted the immunogenicity of the target antigen, leading to the generation of antibodies capable of efficiently neutralizing the viral infection and reducing the number of required doses. Altogether, this study provides a novel perspective for future development of SARS-CoV-2 subunit vaccines by means of lipid-based nanoparticles that can be tested under pre-clinical conditions.

Methods

Animals and ethical statement

Six- to eight-week-old female C57BL/6 mice were maintained under specific pathogen-free conditions at the isogenic mouse facility of the Microbiology Department, University of São Paulo, Brazil. All mice were handled according to procedures approved by the Committee for the Ethical Use of Laboratory Animals from the Institute of Biomedical Sciences of the University of São Paulo (CEUA 6961041120).

Plasmid and protein production

The pCAGGS mammalian expression vector, containing the SARS-CoV-2 S glycoprotein RBD sequence, was obtained from BEI Resources (NIAID, NIH) (NR-52309). The RBD protein was produced in Expi293 cells (Thermo Fisher Scientific Inc., MA, USA) according to the manufacturer's guidelines and purified via single-step His-based affinity chromatography using a HisTrap FF 5 ml column (GE Healthcare, IL, USA). Further details are provided in the Supplementary Materials.

Preparation of lipid nano-multilamellar vesicles (NMVs) loaded with RBD

NMVs were prepared as previously described [20,21], using the following lipids obtained from Avanti Polar Lipids Inc. (AL, USA): dipalmitoyl phosphatidyl choline (DOPC, 850375P), dipalmitoyl phosphatidyl glycine (DPPG, 840455P), dipalmitoyl glycerol succinyl (DGS-NTA(Ni), 790404P), cholesterol (700000), and MPLA (699800). First, DOPC and DPPG phospholipids are suspended in the protein solution and form a lipid bilayer that makes up the inner layer. In this vesicle, the protein can only be incorporated in its hydrophilic portion. The phospholipid DGS-NTA (Ni), present only in the outer vesicle containing also DOPC and CHOL, permits that the histidine tail present in the RBD protein remains bound to the outer surface of the vesicles. The amount of unincorporated protein was measured using the BCA protein assay (Thermo Fisher Scientific Inc., MA, USA).

Dynamic light scattering (DLS) and zeta potential

The polydispersity and volume size distribution of the nanoparticles and proteins were determined via dynamic light scattering (DLS) at 90° (Zetasizer Nano ZS90, Malvern Panalytical Ltd., UK). Measurements were performed in triplicate at 25 °C, and the zeta potential was measured in six replicates.

Evaluation of cell viability

Cell viability was assessed using Cell Proliferation Reagent WST-1 (Roche Applied Science, Mannheim, Germany). Briefly, Vero cells were seeded in a 96-well plate and, upon reaching 70 % confluence, were exposed to the different formulations. After 24 h, the culture medium was replaced and 10 μl of WST-1 reagent was added. Absorbance was measured, after 1 h of incubation, at 440 and 600 nm using a Labsystems Multiskan plate reader (Thermo Fisher Scientific Inc., MA, USA). All assays were performed in six replicates.

Quantification of RBD release from NMVs at different temperatures

The RBD-NMV-MPLA formulations were incubated at 4, 25, and 37 °C. RBD release measurements were performed in triplicate at each temperature over a period of 7 days. NMVs were first separated from the released protein by centrifugation at 15,000 ×*g* for 10 min at 4 °C, after which protein quantification

was performed using the BCA protein assay (Thermo Fisher Scientific Inc., MA, USA).

Mice immunization

Two independent experiments were performed to assess immunogenicity of the vaccine formulations. Five mice were included per vaccine formulation group and received one to three intramuscular immunization doses separated by 2-week intervals. The control groups were injected with saline, while the vaccinated mice received either RBD, RBD-MPLA, RBD-NMV, or the complete RBD-NMV-MPLA formulation. The standard antigen dose was 10 μg/mouse, whereas one group received a single dose of 20 μg. All serum samples were collected 1 day prior to each vaccine dose via submandibular bleeding.

Antibody analyses

An enzyme-linked immunosorbent assay (ELISA) was performed as previously described [26]. Briefly, RBD served as a solid-phase antigen, and the serum obtained from each mouse was serially diluted in duplicate. Immunoenzymatic assays were performed using mouse anti-IgG antibodies conjugated to peroxidase (Sigma-Aldrich, USA). Additionally, IgG subclass responses were assessed using immunized mouse sera treated with anti-IgG1 (Sigma-Aldrich, St. Louis, MO, USA) or anti-IgG2c (SouthernBiotech, Birminghan, USA) antibodies conjugated to peroxidase. To evaluate the strength of antigen-antibody interaction in ELISA, a step involving incubation with increasing concentrations of ammonium thiocyanate (0–4 M), prior to incubation with secondary antibodies (conjugated to peroxidase), was added to the regular protocol.

Intracellular cytokine staining

The splenocyte-derived cytokines were measured using intracellular cytokine staining (ICS), as described in the Supplementary Materials. Briefly, splenocytes were collected 3 weeks after the third immunization and subsequently pulsed with an anti-CD28 agonist antibody (BD Biosciences, USA) in combination with either RBD or a set of 14-mer peptides covering the RBD region in overlap (NR-52402, BEI Resources, USA). After 1 h, the cells were treated with brefeldin A (BD Biosciences, USA) and incubated for 12 h at 37 °C and 5 % CO_2. Non-pulsed cells served as the negative control. Extracellular staining was performed using Live/Dead Fixable Aqua Dead, anti-CD3 BV786 (BioLegend, USA), anti-CD8 APC (BioLegend, USA), and anti-CD4 BV605 (BioLegend, USA). After washing, the fixed and permeabilized cells were intracellularly stained with anti-IFNγ PE (BioLegend, USA), anti-IL-2 BV421 (BioScience), and anti-TNFα Pe-Cy7 (BD Bioscience, USA). The cells were subsequently analyzed using an LSR Fortessa flow cytometer (BD Biosciences, USA).

Viral neutralization test

For this assay, the human viral isolate SARS-CoV-2/human/BRA/SP02cc/2020 (GenBank MT350282.1) was used [27], as described in the Supplementary Materials, and the cytopathic effect (CPE)-based virus neutralization test (VNT) was carried out as previously reported [28]. Briefly, mixtures of SARS-CoV-2 and inactivated pools of immunized mouse serum were added to Vero cells and subsequently incubated for 72 h, before plate assessment for the presence or absence of CPE-VNT. Neutralizing antibody titers correspond to the highest serum dilution capable of fully neutralizing virus growth. In accordance with the World Health Organization recommendations [29], all procedures involving SARS-CoV-2 were performed in a biosafety level 3 laboratory located at the Instituto de Ciências Biomédicas, USP, Brazil.

Immunofluorescence of SARS-CoV-2-infected Vero cells determined using sera from immunized mice

Immunofluorescence assays were performed as previously described [30,31] and as detailed in the Supplementary Materials. Briefly, Vero cells were infected with SARS-CoV-2 (GenBank MT350282.1) at a 0.1 multiplicity of infection (MOI), followed by a 72 h incubation period. The infection was detected using inactivated pools of immunized mouse serum, which were stained with Alexa488-conjugated goat anti-mouse IgG (Thermo Fisher Scientific Inc., MA, USA) and DAPI (4,6-diamidino-2-phenylindole; Sigma-Aldrich, St. Louis, MO, USA). Image acquisition was performed using the Operetta High Content Imaging System (PerkinElmer, Waltham, MA, USA).

Statistical analysis

Statistical analyses were performed using Prism 9 (GraphPad Software, USA) and included a two-way analysis of variance (ANOVA), followed by a *t*-test corrected for multiple comparisons (post-test Bonferroni correction). *P*-values below 0.05 were considered statistically significant. All values are reported either as individual values or as mean ± SD.

Results

Characterization of NMV-based formulations

Recombinant SARS-CoV-2 RBD was produced in Expi293 cells, which demonstrated high recovery yields and near-native conformation and glycosylation patterns. A highly pure protein was obtained with single-step nickel-based affinity chromatography and exhibited the expected electrophoretic mobility (Fig. 1A). The purified RBD was incorporated into NMV formulations in the inner and outer membrane layers, as illustrated in Fig. 1S. The RBD incorporation efficiency reached 96.6 %, with a protein distribution ratio of 0.19 in the outside/inside lipid layers. Moreover, MPLA was also incorporated into both layers of the NMVs. A multimodal distribution was observed for the RBD-loaded NMVs, which demonstrated three distinct vesicle populations with mean diameters of 51.2, 106.8, and 216.8 nm (Fig. 1B). Zeta potential analyses indicated a negative nanoparticle surface charge of −17.5 mV and an overall high polydispersity index of 0.92. Antigen release from the loaded NMVs was temperature-dependent, demonstrating enhanced kinetics at higher temperatures (Fig. 1C). Accordingly, formulations maintained at 37 °C released >50 % of the loaded protein
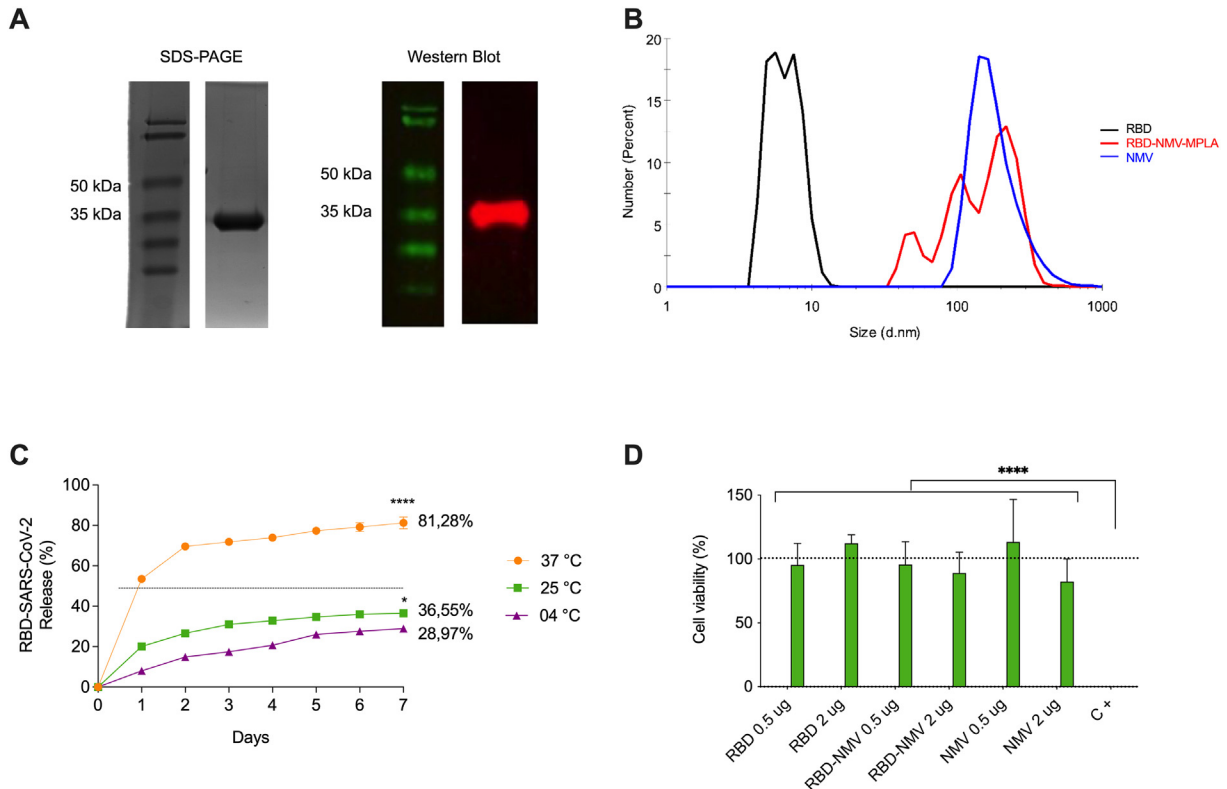
Fig. 1. Production of recombinant SARS-CoV-2-derived RBD protein in mammalian cells and characterization of the vaccine formulation based on NMVs. (A) Immunodetection of the expression of purified RBD via western blotting (WB). (B) Determination of nanoparticle diameter via dynamic light scattering (DLS). Values correspond to the mean of the diameters obtained in three replicates. (C) Time-course measurement of RBD release from NMVs at different temperatures. Values represent the mean ± SE of values from experiments performed in triplicate for each temperature. Statistical differences are indicated regarding samples kept at 4 °C. ****$p < 0.0001$ (*t*-test). (D) Cellular viability of Vero cells incubated with RBD-NMV-MPLA after 24 h, as assessed using WST. The values represent the means ± SE of the absorbance values determined in six replicates of each vaccination formulation. Statistically significant differences are indicated in the graph. ****p < 0.0001 for two-way ANOVA with Bonferroni's post-test correction is indicated in relation to the negative control.

on the first day, while formulations maintained at lower temperatures (25 °C and 4 °C) released <40 % of the loaded protein after a 7-day incubation period.

Lastly, no statistically significant impact on Vero cells viability was observed following the 24 h incubation period with the tested proteins and NMV concentrations, indicating negligible toxicity to mammalian cells (Fig. 1 D).

Analysis of the humoral responses

Immunogenicity was first evaluated using C57BL/6 mice that were immunized intramuscularly with 10 μg of either the RBD-MPLA combination or with the NMV-based formulation (RBD-NMV-MPLA). The vaccination regimen comprised two doses administered 2 weeks apart (Fig. 2 A). Furthermore, NMVs have been reported to promote vaccine depot effects [21]. Thus, we included an additional immunization group that was administered a single dose containing twice the amount of the target antigen (20 μg). Mice included in the control group were injected with saline, and the corresponding results were subtracted from that obtained from the immunized groups. As shown in Fig. 2B, antigen assembly into nanoparticles resulted in a significant increase in antigen-specific IgG titers. Notably, the single-dose regimen demonstrated significantly lower antibody titers com-

pared to the two-dose regimen, indicating that the prime/boost immunization regimen is more efficient than the putative depot effect obtained with the single-dose regimen.

The analysis of IgG subclass responses (Fig. 2 C) suggested that although the presence of NMV had no significant impact on IgG1 titers, it directly increased the antigen-specific IgG2c responses, thus promoting a balanced IgG subclass response with a slightly polarized Th1 profile. ELISA was performed in the presence of a dissociating agent (ammonium thiocyanate) and demonstrated a prominent increase in the antigen-antibody avidity in mice immunized with the antigen-loaded NMVs (Fig. 2 D).

Immunofluorescence was used to investigate the binding capacity of antibodies raised in mice immunized to the SARS-CoV-2 virus. The infected cells were exposed to serially diluted serum samples collected from mice immunized with two doses of either RBD-MPLA or RBD-NMV-MPLA. As depicted in Fig. 3, sera from RBD-MPLA immunized mice failed to bind to the virus particles present in infected cells, whereas sera from the RBD-NMV-MPLA immunized mice successfully bound to SARS-CoV-2 virus particles up to a dilution of 1:320. These results clearly demonstrate the potential of NMV incorporation to result in the induction of efficient antibody responses.
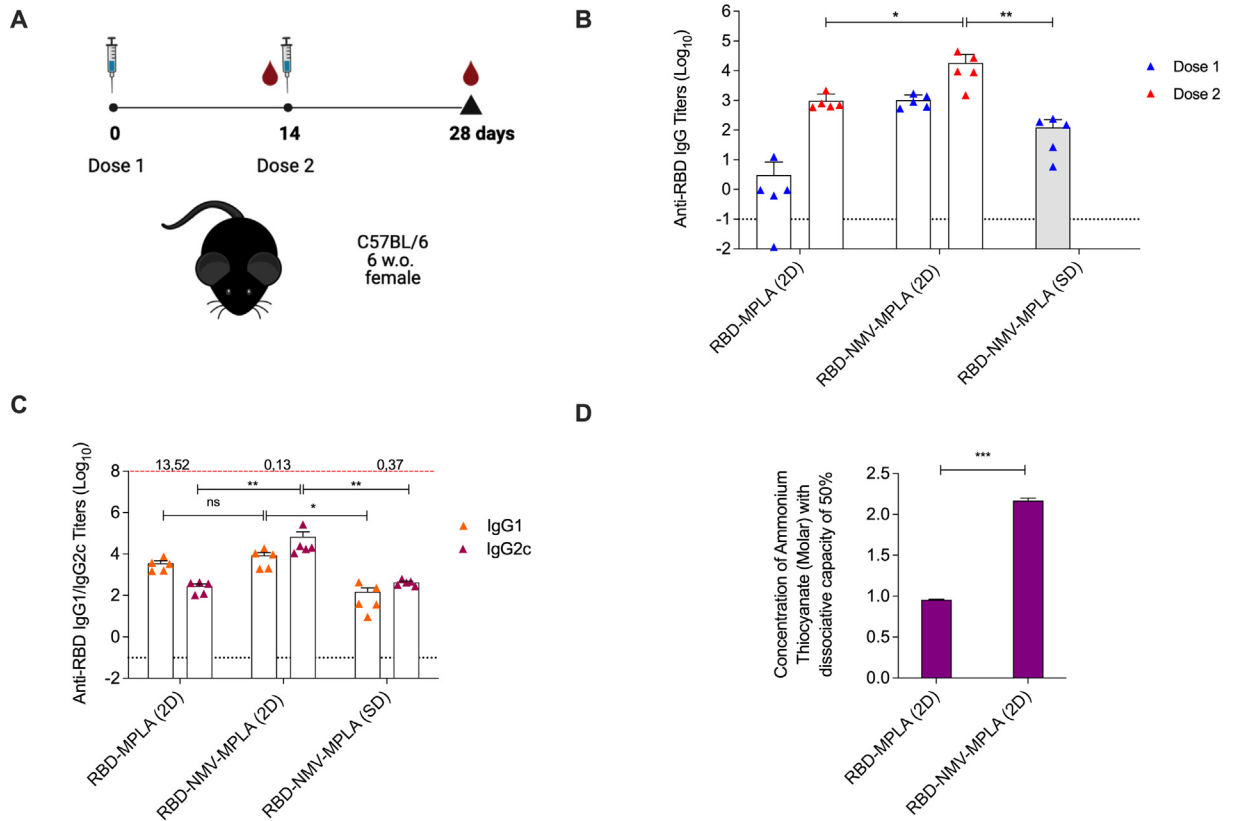
Fig. 2. Immunization with RBD-NMV-MPLA induces strong humoral responses in vaccinated mice. (A) Two-dose vaccination regimens, indicated as 2D, of C57BL/6 mice immunized with 10 μg of antigen per dose, or a single dose (20 μg), indicated as 1D. Serum samples were collected 14 days after each dose. (B) Anti-RBD-specific total IgG titers. (C) Anti-RBD IgG1 and IgG2c subclass titers. Values above the dashed red line correspond to the mean IgG1/IgG2c titer ratio. The values obtained in the control group were subtracted from the values obtained in the experimental groups (Mean ± 2 × SD). (D) Antigen affinity for RBD-specific antibodies after incubation with different ammonium thiocyanate concentrations could dissociate 50 % of the bound antibodies. Antigen affinity values represent the means ± SE of values from experiments performed in duplicate. Statistical differences are indicated in the graphs. ns: not significant; ***$p <$ 0.001; **$p <$ 0.01; *$p <$ 0.05, as determined using a two-way ANOVA with Bonferroni's post-test correction.
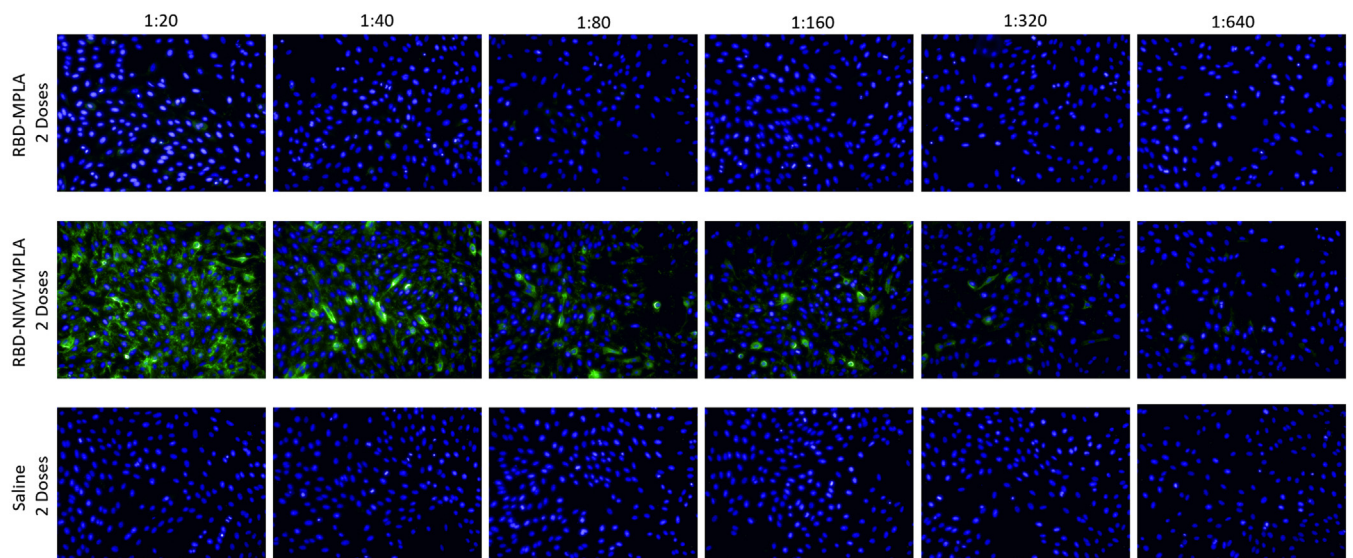

Fig. 3. Binding of anti-RBD antibodies raised in vaccinated mice to SARS-CoV-2 virus particles. Vero cells infected for 72 h with SARS-CoV-2 were incubated with different dilutions of serum samples collected after the second vaccine dose. Images captured on Operetta.

To this point, the evaluated parameters represent an indirect demonstration of the quality of the induced antigen-specific antibodies. Therefore, we performed VNTs, which provide a highly accurate indication of antibody effectiveness, using a SARS-CoV-2 strain (Wuhan, China) isolated from the first Brazilian patient infected with the virus in 2020 [27]. The VNT_{100} results indicated the maximum dilution of antibodies in which complete neutralization was obtained, with a threshold value of 20 considered significant. The results obtained here demonstrated that while the RBD-MPLA immunized mouse serum induced a significant humoral response, the resulting antibodies failed to neutralize SARS-CoV-2 in vitro, with a $VNT_{100} < 20$ (Table 1). Nonetheless, mice immunized with RBD-NMV-MPLA produced antibodies with a strong virus-neutralizing activity that could block viral infection in vitro up to a dilution of 1:320.

Effects of RBD-NMV-MPLA components on immunogenicity of the vaccine formulation

Results obtained during the initial immunization experiment demonstrated that the RBD-NMV-MPLA formulation provided a promising vaccine strategy against SARS-CoV-2. Next, the contribution of each of the three vaccine formulation components to the induction of immune responses was assessed. This was done by immunizing mice with RBD, RBD mixed either with MPLA or NMV, or with the complete formulation (RBD-NMV-MPLA). As described previously, the control group was injected with saline, and antibody titer results were obtained following deduction calculations. A three-dose vaccination regimen was employed with the hypothesis that an additional dose may further increase the ensuing IgG and virus neutralization titers (Fig. 4 A).

Analysis of total serum IgG titers (Fig. 4 B) indicated that RBD is a highly immunogenic antigen capable of inducing elevated antibody titers following a three-dose vaccine regimen. However, RBD incorporated into NMVs displayed no significant difference between IgG titers obtained after two or three doses, regardless of MPLA addition, emphasizing the inherent adjuvant effects of NMVs. Furthermore, the RBD-MPLA-immunized mice required three doses to reach antibody levels comparable to those obtained with two doses of the NMV-containing formulations. Collectively, these results suggest that the inclusion of MPLA had a negligible impact on the immunogenicity (IgG titers) of the NMV vaccine formulation. In addition, incorporation of RBD into NMVs allowed for maximum antigen-specific antibody titers after only two doses.

Analyses of IgG subclass responses showed that NMVs and MPLA affected the induced antibody responses. While RBD alone induced a strong polarization towards IgG1 (IgG1/IgG2c ratio of 1046), its incorporation into NMVs induced a more balanced IgG subclass response. The latter is indicated by the distinct induction of IgG2c (Fig. 4 C), resulting in a reduced IgG1/IgG2c ratio of 2.36 (RBD-NMV) and 0.75 (RBD-NMV-MPLA).

Regarding antigen-binding avidity, the dissociation of RBD-specific antibodies with ammonium thiocyanate revealed that while addition of MPLA and NMV individually contributed to an increase in avidity, both components acted synergistically in the promotion of antibody-antigen avidity (Fig. 4 D). These results indicated that although total IgG titers were statistically similar in mice immunized with either NMV, MPLA, or a combination of both, major differences were observed in the induced subclass profiles and antigen avidity.

Next, the ability of the antibodies elicited in mice immunized with different vaccine formulations to neutralize SARS-CoV-2 was assessed. The three-dose immunization regimen with RBD alone was not capable of inducing neutralizing antibodies. Similarly, the mice immunized with RBD and NMV generated antibodies with a low virus neutralization titer (VNT_{100} reverse titer of 20), while mice immunized with RBD-MPLA generated antibodies with a VNT_{100} of 180 after three doses (Table 1). In contrast, mice immunized with the complete vaccine formulation (RBD-NMV-MPLA) produced significant virus-neutralizing antibody titers at maximal values after a two-dose regimen (320–640), indicating that antigen incorporation into adjuvanted nanoparticles promoted antibody induction without the need for

Table 1
Evaluation of the neutralizing effect of antigen-specific IgG antibodies by cytopathic effect (VNT).

Formulation[a]	Immunization[b]	VNT100[c] Dose 1	VNT100[d] Dose 2	VNT100[e] Dose 3
RBD-MPLA (2 doses)	1	–	<20	–
RBD-NMV-MPLA (2 doses)	1	–	320	–
Saline (2 doses)	1	–	<20	–
RBD-NMV-MPLA (1 dose)	1	<20	–	–
RBD (3 doses)	2	–	<20	<20
RBD-MPLA (3 doses)	2	–	<20	180
RBD-NMV (3 doses)	2	–	<20	20
RBD-NMV-MPLA (3 doses)	2	–	640	320
Saline (3 doses)	2	–	<20	<20

Different dilutions of sera after the first, second, and third doses of mice immunized from 1:20 onwards were incubated with MOIs 0 and 1 of SARS-CoV-2 and subsequently added to a monolayer of Vero cells. After incubation for 72 h, the cytopathic effects at the different tested dilutions were observed using an inverted microscope.

[a] Experimental vaccine formulations.
[b] Immunization experiments based on a two (1) or three (2) dose regimen.
[c] Neutralizing effect of sera after single-dose immunization.
[d] Neutralization effect of sera after the second dose
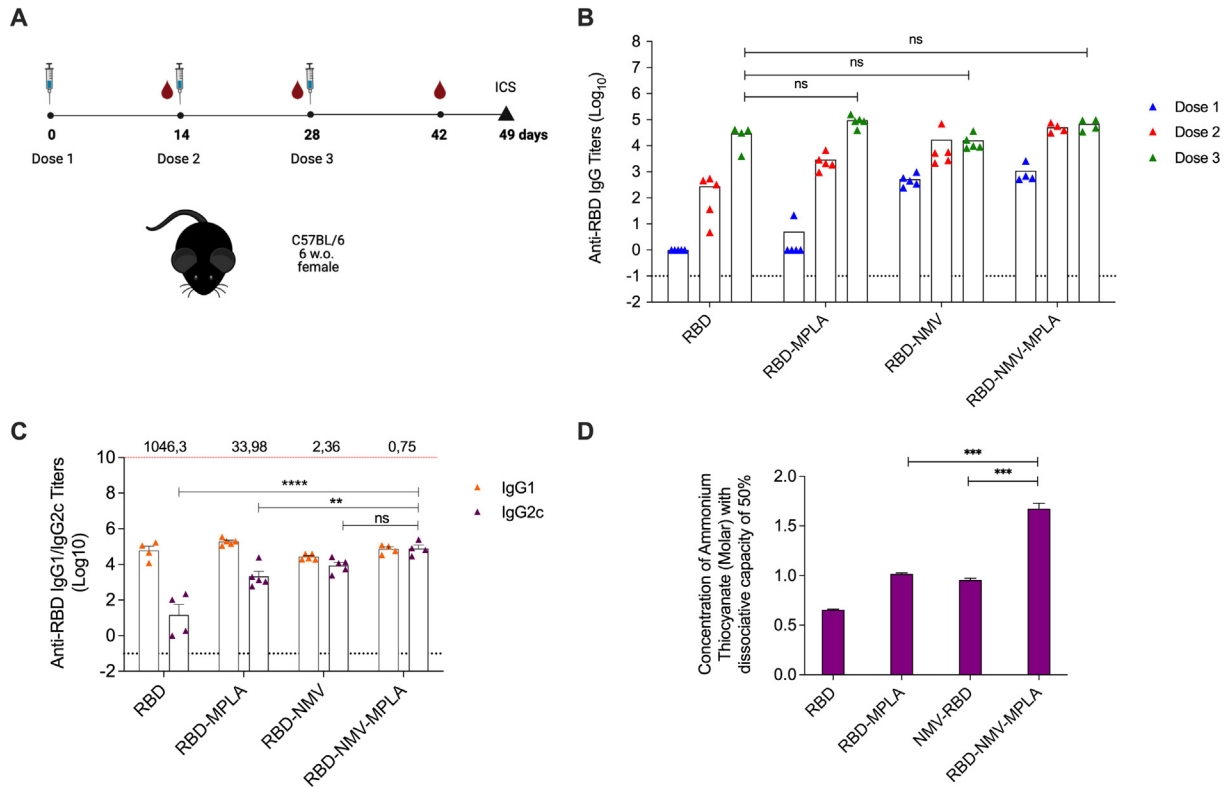[e] Neutralization effect of sera after the third dose.

Fig. 4. Roles of NMVs and MPLA in the induction of humoral responses in mice immunized with RBD-NMV-MPLA. (A) Schematic representation of the three-dose vaccine regimen. (B) RBD-specific IgG titers. (C) RBD-specific serum IgG subclass responses. Values above the dashed red line correspond to the mean IgG1/IgG2c titer ratio. (D) Antigen affinity of RBD-specific antibodies after incubation with different ammonium thiocyanate concentrations could dissociate 50 % of the bound antibodies. In total IgG and subclass analyses, the values obtained in the control group were subtracted from the values obtained in the experimental groups (means ± 2 × SD). The antibody titers represent the mean ± SD of the individual titers determined in duplicate for each dose. Individual values are indicated by triangles. In the antigen affinity determination, the values represent the mean ± SE of values from experiments performed in duplicate. Statistical differences are indicated in the graphs. ns: not significant; ****$p < 0.0001$; ***$p < 0.001$; **$p < 0.01$, as determined via a two-way ANOVA with Bonferroni's post-test correction.

additional booster doses. Notably, no significant signs of morbidity, such as bristling hairs, curved spine or paralyzed legs, and any additional signs of physical pain including closed eyes and slowness, were observed in mice subjected to either the two- or three-dose vaccine regimens or the different tested vaccine formulations (data not shown).

Analysis of the cellular (T cell) responses

Our results demonstrate that the RBD-NMV-MPLA vaccine formulation is capable of inducing significant virus-neutralizing antibody responses. Lastly, the concomitant activation of antigen-specific T-cell responses in vaccinated mice was assessed via intracellular cytokine staining (ICS). No significant results were observed for mice subjected to the two-dose vaccine regimen. The production of IL-2, TNF-α, and IFN-ɣ by CD4+ and CD8+ T cells was analyzed using splenocytes collected 3 weeks after the third vaccine dose (Fig. 5A–F). Splenocytes were exposed to 3 different conditions: stimulated with the purified RBD (labeled as "RBD" in the x axis of graphs on Fig. 5A-F), stimulated with a peptide pool covering the complete RBD sequence (labeled as "pep" in the x axis of graphs on Fig. 5A-F), and in addition, a non-stimulated group serving as the negative control

(labeled as "C −" in the x axis of graphs on Fig. 5A-F). The results demonstrated that only MPLA-containing vaccine formulations were capable of inducing RBD-specific immune cell responses. The lack of significant differences between unstimulated and stimulated cells suggests that RBD and RBD-NMV formulations do not induce specific T-cell activation. Furthermore, no significant cytokine differences were observed between RBD-MPLA- and RBD-NMV-MPLA-immunized mice, suggesting that the activation of T cell-dependent responses is ascribed to the presence of MPLA.

Discussion

One positive impact associated with the COVID-19 pandemic was the unparalleled advances observed in the development of new vaccine formulations in a short period of time. Such advances included the deployment of new vaccine technologies, such as those based on messenger RNA and the adenovirus-vectored vaccines [5–11]. Nonetheless, unmatched challenges, such as the need to induce long lived protection and activation of broader protective immune responses capable of facing the inherent natural variability of coronaviruses, demands further technological improvements.
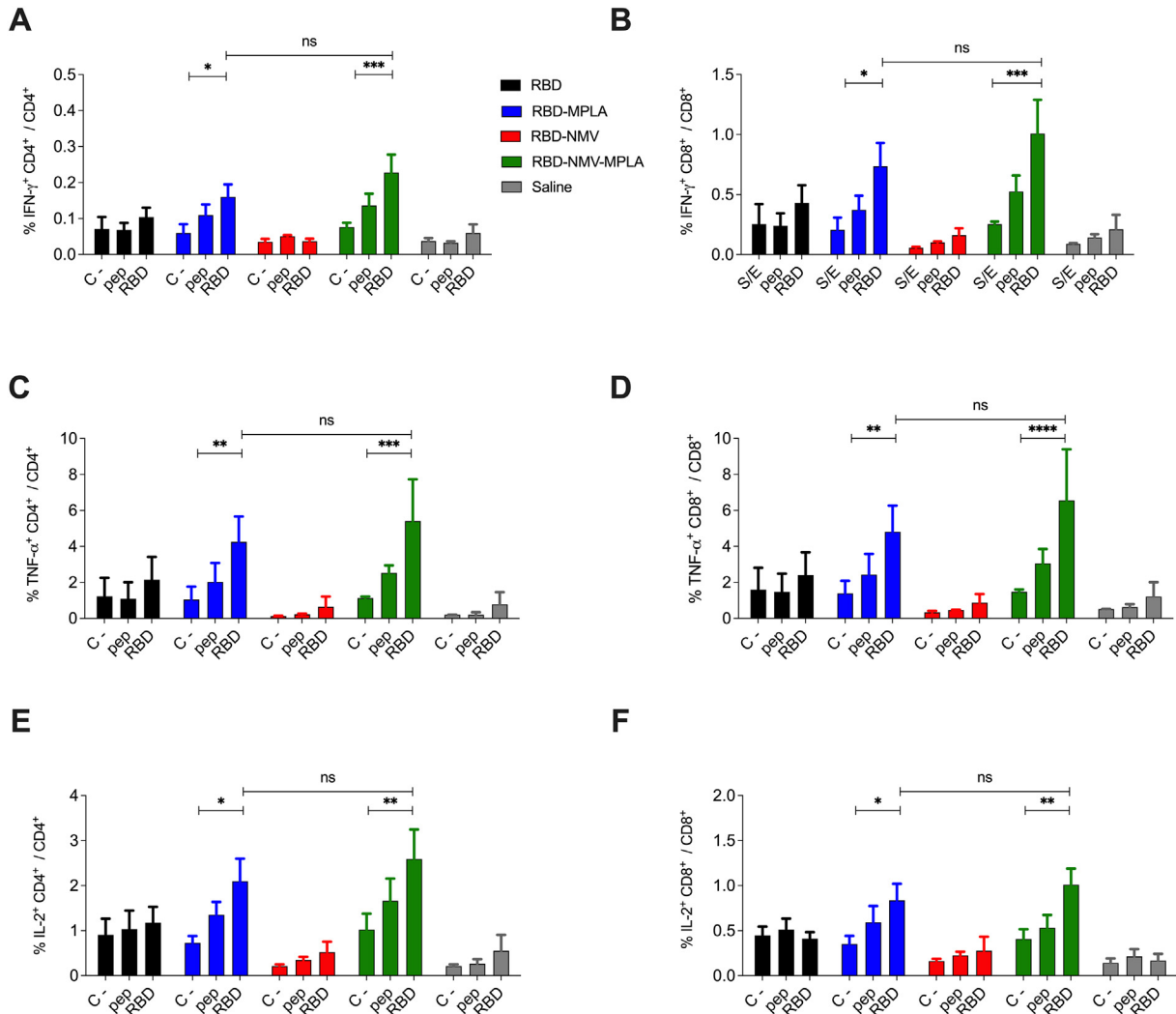
Fig. 5. RBD-NMV-MPLA vaccine induced antigen-specific CD4+ and CD8+ T-cell responses. Spleen cells of immunized mice were collected and exposed to 3 different conditions: stimulated with the purified RBD (labeled as "RBD"), stimulated with a peptide pool covering the complete RBD sequence (labeled as "pep"), and in addition, a non-stimulated group serving as the negative control (labeled as "C −"). The induced cytokine responses were measured using ICS assays and flow cytometry. Data based in one experiment correspond to means ± SD of two pools of splenocytes for each tested experimental group performed in triplicate. Statistical differences are indicated in the graphs. ns: not significant; **** p < 0.0001; ***p < 0.001; **[< 0.01; *p < 0.05, as determined via a two-way ANOVA with Bonferroni's post-test correction.

The incorporation of protein antigens into lipid nanoparticles is a well-known approach to enhance mammalian immune responses by particularly influencing the activation of antibody-producing cells [32]. Here, we evaluated an immunization strategy based on NMVs that allows coupling of antigens and adjuvants at both the outer and inner NMV lipid layers [19–21]. Various vaccine formulations were produced from combinations of a SARS-CoV-2-derived recombinant antigen (RBD) and an adjuvant (MPLA) incorporated into NMVs. The results demonstrated that although all formulations were capable of inducing high serum antibody titers, disparities were present regarding the quality of antigen-specific antibodies raised in mice immunized with the complete vaccine formulation (RBD-NMV-MPLA). Antibodies raised in RBD-NMV-MPLA-immunized mice were able to bind and neutralize viral particles after two vaccine doses. Additionally, the presence of MPLA and NMV modulated an-

tigen-specific antibody avidity and serum IgG subclass responses. Interestingly, the incorporation of MPLA into NMVs induced higher cellular immune responses, as determined by the presence of specific cytokines produced by CD8+ and CD4+ T cells. Altogether, these results support the use of adjuvanted NMVs as a technological platform for the generation of subunit vaccines using purified recombinant proteins, including, but not limited to, vaccines against COVID-19.

The use of an RBD as an antigen is evident when considering that it constitutes the S protein region responsible for binding to host cell receptors and mediating virus entry into cells [13]. The recombinant RBD was incorporated in both inner and outer layers of the NMVs, resulting in nanoparticles with a multimodal size distribution encompassing three populations of 50–200 nm in diameter. This is consistent with previous reports, which indicated that NMVs display an average size of 50 nm under cryo-

TEM but tend to aggregate by self-attraction forces into small clusters that appear larger upon DLS [33]. The observed size range of the RBD-loaded NMVs was of particular interest, considering that it would avoid renal clearance, characteristic of nanoparticles <5 nm, while remaining in the appropriate size range that allows efficient draining to lymphoid organs and, consequently, phagocytosis by antigen-presenting cells that may present the target antigen epitopes to effector immune cells [34].

The RBD-loaded NMV formulations showed moderate stability at lower temperatures but released >50 % of the protein at physiological temperatures after 24 h. Despite previous in vivo observations that NMVs could promote a moderate depot effect [21], the current results demonstrated that single-dose immunization containing a twofold antigen load, combined with the fast antigen release exhibited at 37 °C, did not support a significant booster effect on the induced antibody responses. Nonetheless, it is noteworthy that NMVs did not show any clear toxic effects either in vitro or in vivo in any vaccine formulation.

The initial two-dose regimen was aimed at establishing whether the presence of NMVs would impact the quantity and/or quality of the induced antibody responses. In accordance with previous reports [20,21], our results indicated that the RBD-NMV-MPLA formulation was capable of inducing higher antibody titers than the RBD-MPLA formulation. Additionally, the NMV-containing formulations induced a more balanced IgG subclass response and induction of IgG2c, which was not observed in mice immunized with RBD-MPLA, thereby indicating probable activation of both cellular (T cell) and humoral (B cell) responses via NMV incorporation. NMVs also had a major impact on antigen-antibody binding avidity, higher than the one observed for the RBD-MPLA. Our results demonstrate that, similar to what has been extensively described for adjuvants, nanoparticles can also modulate the immune response, which is maximized when administered in combination with adjuvants [35–37]. Altogether, these results substantiate the notion that the combination of recombinant purified antigens with adjuvanted NMVs affects both the magnitude and quality of the induced antigen-specific immune responses.

Sera from RBD-NMV-MPLA immunized mice could bind to and detect SARS-CoV-2 particles in infected cells, whereas sera from RBD-MPLA immunized mice failed to do so. This is particularly relevant because the antibodies elicited in mice immunized with antigens organized into different kinds of nanoparticles may show an impaired ability to bind native proteins [26]. As such, the results generated here validate the use of the NMV-MPLA platform for the generation of subunit vaccines capable of preserving the conformational and immunological features of the target virus antigen. Furthermore, sera from RBD-NMV-MPLA immunized mice neutralized SARS-CoV-2 in vitro up to a reverse titer of 320–640, while sera from RBD-MPLA immunized mice did not show a significant virus neutralization titer (<20). These results confirmed that a two-dose regimen was sufficient to induce significant serum levels of protective antibodies in mice immunized with RBD-NMV-MPLA.

In addition, we sought to determine the contribution of each vaccine formulation component (NMV and MPLA) to the induction of antigen-specific antibody responses. Incorporation of either NMVs or MPLA did not boost the RBD-specific IgG responses in mice immunized with purified RBD. Similarly, no synergistic effects regarding the induction of RBD-specific antibodies were demonstrated in mice immunized with RBD-NMV-MPLA compared to mice immunized only with RBD. Nonetheless, a more detailed analysis of the serum IgG responses revealed that the IgG subclass varied among the immunization groups. The RBD-immunized mice developed a strong IgG1 polarization, while mice immunized with NMV-containing formulations displayed a more balanced response with a notable induction of an IgG2c response. Despite IgG titer results, mice immunized with RBD combined with either MPLA or NMV-MPLA were capable of inducing significantly higher VNT_{100} titers. Indeed, MPLA is an FDA-approved adjuvant that binds TLR-4 receptors and boosts immune responses either towards Th1 or a balanced Th1/Th2 response, depending on the chosen antigen and administration route [38]. Collectively, the results based on a 3-dose regimen revealed the high immunogenicity associated with recombinant RBD in mice, and that the addition of NMVs and/or MPLA had a significant impact on the quality of the induced antibody responses, particularly regarding the capacity to recognize and block the binding of RBD to host cell receptors.

Subunit vaccines are generally poor inducers of T cell-based immune responses [39]. Despite no significant results being observed in mice subjected to a two-dose regimen, mice immunized with three vaccine doses clearly demonstrated activation of both $CD8^+$ and $CD4^+$ T cells, particularly in RBD-MPLA- and RBD-NMV-MPLA-immunized mice. Interestingly, our results demonstrated that T-cell activation is dependent on MPLA incorporation into the vaccine formulation.

Our results demonstrate that the incorporation of recombinant RBD and MPLA into NMVs represents a novel strategy for developing vaccine formulations endowed with the ability to enhance serum antigen-specific antibody and T-cell responses. The incorporation of both antigen and MPLA into NMVs is necessary to modulate the quality of the induced antibody responses, including higher antigen avidity, modulation of IgG subclass responses, and activation of antigen-specific T-cell responses, as previously reported by our group [20,21]. Notably, the generation of virus-neutralizing antibodies was improved after the incorporation of purified RBD into NMVs. Generation of virus-neutralizing antibodies usually requires the maintenance of a structural conformation in which nonlinear epitopes are recognized by neutralizing antibodies. In this sense, the multimeric presentation of RBD on the surface of NMVs may mimic the tight and well-ordered conformation found in virions, which are recognized by both innate (antigen-presenting cells) and acquired (B and T cells) components of the mammalian immune system. Taken together, our results demonstrate that by adding a viral antigen (RBD) to MPLA-containing NMV we achieved a boost in the induction of serum antibody responses, which included not only quantitative enhancement of the response but also modulation of antigen affinity and IgG subclass responses. Altogether, these effects resulted in the induction of a stronger virus neutralization response that allowed reduction of the number of vaccine doses. Overall, this study highlights that IgG titers alone are not sufficient when comparing different vaccine formulations and demonstrates that the combination of lipid nanoparticles and a lipid adjuvant displays synergic effects that enhance antigen capacity for the induction of immune responses.

CRediT authorship contribution statement

Monica Josiane Rodrigues-Jesus: Conceptualization, Methodology, Investigation, Validation, Data curation, Writing – original draft, Writing – review & editing. **Marianna Teixeira de Pinho Favaro:** Conceptualization, Methodology, Investigation, Validation, Data curation, Writing – original draft, Writing – review & editing. **Aléxia Adrianne Venceslau-Carvalho:** Investigation, Methodology. **Maria Fernanda de Castro-Amarante:** Investigation, Methodology, Writing – original draft. **Bianca da Silva Almeida:** Investigation, Methodology, Writing – original draft. **Mariângela de Oliveira Silva:** Investigation, Methodology, Writing – original draft. **Robert Andreata-Santos:** Investigation, Methodology, Validation, Writing – review & editing. **Cecilia Gomes Barbosa:** Investigation, Methodology, Writing – original draft. **Samantha Carvalho Maia Brito:** Investigation, Methodology. **Lucio H. Freitas-Junior:** Conceptualization, Visualization. **Silvia Beatriz Boscardin:** Conceptualization, Methodology, Visualization, Supervision, Writing – review & editing. **Luís Carlos de Souza Ferreira:** Conceptualization, Funding acquisition, Visualization, Supervision, Project administration, Writing – original draft, Writing – review & editing.

Acknowledgements

Appendix A. Supplementary data

Supplementary data to this article can be found online at https://doi.org/10.1016/j.nano.2022.102595.

References

1. Zhu N, Zhang D, Wang W, et al. A novel coronavirus from patients with pneumonia in China, 2019. *N Engl J Med* 2020;**382**(8):727-33.
2. *Weekly Epidemiological Update on COVID-19 - 15 March*; 2022https://www.who.int/publications/m/item/weekly-epidemiological-update-on-covid-19—15-march-2022.
3. Anderson RM, Vegvari C, Hollingsworth TD, et al. The SARS-CoV-2 pandemic: remaining uncertainties in our understanding of the epidemiology and transmission dynamics of the virus, and challenges to be overcome. *Interface Focus* 2021;**11**(6).
4. Koelle K, Martin MA, Antia R, Lopman B, Dean NE. The changing epidemiology of SARS-CoV-2. *Science (80-)* 2022;**375**(6585):1116-21.
5. Polack FP, Thomas SJ, Kitchin N, et al. Safety and efficacy of the BNT162b2 mRNA Covid-19 vaccine. *N Engl J Med* 2020;**383**(27):2603-15.
6. Baden LR, El Sahly HM, Essink B, et al. Efficacy and safety of the mRNA-1273 SARS-CoV-2 vaccine. *N Engl J Med* 2021;**384**(5):403-16.
7. Voysey M, Costa Clemens SA, Madhi SA, et al. Single-dose administration and the influence of the timing of the booster dose on immunogenicity and efficacy of ChAdOx1 nCoV-19 (AZD1222) vaccine: a pooled analysis of four randomised trials. *Lancet (London, England)* 2021;**397**(10277):881-91.
8. Logunov DY, Dolzhikova IV, Shcheblyakov DV, et al. Safety and efficacy of an rAd26 and rAd5 vector-based heterologous prime-boost COVID-19 vaccine: an interim analysis of a randomised controlled phase 3 trial in Russia. *Lancet (London, England)* 2021;**397**(10275):671-81.
9. Kim JH, Marks F, Clemens JD. Looking beyond COVID-19 vaccine phase 3 trials. *Nat Med* 2021;**27**(2):205-11.
10. Heath PT, Galiza EP, Baxter DN, et al. Safety and efficacy of NVX-CoV2373 Covid-19 vaccine. *N Engl J Med* 2021;**385**(13):1172-83.
11. Sapkal GN, Yadav PD, Ella R, et al. *Neutralization of UK-variant VUI-202012/01 With COVAXIN Vaccinated Human Serum*. bioRxiv; 2021. 2021.01.26.426986.
12. Yadav R, Chaudhary JK, Jain N, et al. Role of structural and non-structural proteins and therapeutic targets of SARS-CoV-2 for COVID-19. *Cells* 2021;**10**(4).
13. Tai W, He L, Zhang X, et al. Characterization of the receptor-binding domain (RBD) of 2019 novel coronavirus: implication for development of RBD protein as a viral attachment inhibitor and vaccine. *Cell Mol Immunol* 2020;**17**(6):613-20.
14. Lee S, Nguyen MT. Recent advances of vaccine adjuvants for infectious diseases. *Immune Netw* 2015;**15**(2):51-7.
15. Schmidt ST, Foged C, Korsholm KS, Rades T, Christensen D. Liposome-based adjuvants for subunit vaccines: formulation strategies for subunit antigens and immunostimulators. *Pharmaceutics* 2016;**8**(1):1-22.
16. Fries CN, Curvino EJ, Chen JL, Permar SR, Fouda GG, Collier JH. Advances in nanomaterial vaccine strategies to address infectious diseases impacting global health. *Nature Nanotechnology* 2021;**16**:385-98.
17. Moon JJ, Suh H, Bershteyn A, et al. Interbilayer-crosslinked multi-lamellar vesicles as synthetic vaccines for potent humoral and cellular immune responses. *Nat Mater* 2011;**10**(3):243-51.
18. DeMuth PC, Moon JJ, Suh H, Hammond PT, Irvine DJ. Releasable layer-by-layer assembly of stabilized lipid nanocapsules on microneedles for enhanced transcutaneous vaccine delivery. *ACS Nano* 2012;**6**(9):8041-51.
19. Genito CJ, Beck Z, Phares TW, et al. Liposomes containing monophosphoryl lipid a and QS-21 serve as an effective adjuvant for soluble circumsporozoite protein malaria vaccine FMP013. *Vaccine* 2017;**35**(31):3865-74.
20. Rodrigues-Jesus MJ, Fotoran WL, Cardoso RM, Araki K, Wunderlich G, Ferreira LCS. Nano-multilamellar lipid vesicles (NMVs) enhance protective antibody responses against Shiga toxin (Stx2a) produced by enterohemorrhagic Escherichia coli strains (EHEC). *Braz J Microbiol* 2019;**50**(1):67-77.
21. Venceslau-Carvalho AA, de Pinho Teixeira, Favaro M, Ramos Pereira L, et al. Nano-multilamellar lipid vesicles loaded with a recombinant form of the chikungunya virus E2 protein improve the induction of virus-neutralizing antibodies. Nanomedicine nanotechnology. *Biol Med* 2021;**37**102445.
22. Coccia M, Collignon C, Hervé C, et al. *Cellularand Molecular Synergy in AS01-adjuvanted Vaccines Results in an Early IFNγ ResponsePromoting Vaccine Immunogenicity*, 2. ; 2017. p. 25.

23. Givord C, Welsby I, Detienne S, et al. Activation of the endoplasmic reticulum stress sensor IRE1α by the vaccine adjuvant AS03 contributes to its immunostimulatory properties. *npj Vaccines* 2018;**3**(1):20.

24. Rudra JS, Sun T, Bird KC, et al. Modulating adaptive immune responses to peptide self-assemblies. *ACS Nano* 2012;**6**(2):1557-64.

25. Pejawar-Gaddy S, Kovacs JM, Barouch DH, Chen B, Irvine DJ. Design of lipid nanocapsule delivery vehicles for multivalent display of recombinant env trimers in HIV vaccination. *Bioconjug Chem* 2014;**25**(8):1470-8.

26. Favaro MTP, Rodrigues-Jesus MJ, Venceslau-Carvalho AA, et al. Nanovaccine based on self-assembling nonstructural protein 1 boosts antibody responses to zika virus. *Nanomedicine nanotechnologyBiol Med* 2021;**32**(2021)102334.

27. Araujo DB, Machado RRG, Amgarten DE, et al. SARS-CoV-2 isolation from the first reported patients in Brazil and establishment of a coordinated task network. *Mem Inst Oswaldo Cruz* 2020;**115**:1-8.

28. Pardi N, Hogan MJ, Pelc RS, et al. Zika virus protection by a single low-dose nucleoside-modified mRNA vaccination. *Nature* 2017;**543**(7644):248-51.

29. Wendel S, Kutner JM, Machado R, et al. Screening for SARS-CoV-2 antibodies in convalescent plasma in Brazil: preliminary lessons from a voluntary convalescent donor program. *Transfusion* 2020;**60**(12):2938-51.

30. Franco CH, Alcântara LM, Chatelain E, Freitas-Junior L, Moraes CB. Drug discovery for chagas disease: impact of different host cell lines on assay performance and hit compound selection. *Trop Med Infect Dis* 2019;**4**(2).

31. Freire MCLC, Noske GD, Bitencourt NV, et al. Non-toxic dimeric peptides derived from the bothropstoxin-I are potent SARS-CoV-2 and papain-like protease inhibitors. *Molecules* 2021;**26**(16).

32. Bachmann MF, Jennings GT. Vaccine delivery: a matter of size, geometry, kinetics and molecular patterns 1011 *Nat Rev Immunol* 2010;**10**(11):787-96 2010.

33. Fotoran WL, Müntefering T, Kleiber N, et al. A multilamellar nanoliposome stabilized by interlayer hydrogen bonds increases antimalarial drug efficacy. *Nanomedicine Nanotechnology, Biol Med* 2019;**22**.

34. Luo M, Samandi LZ, Wang Z, Chen ZJ, Gao J. Synthetic nanovaccines for immunotherapy. *J Control Release* 2017;**263**:200-10.

35. Maeda DLNF, Batista MT, Pereira LR, et al. Adjuvant-mediated epitope specificity and enhanced neutralizing activity of antibodies targeting dengue virus envelope protein. *Front Immunol* 2017;**8**(SEP):1175.

36. Bielinska AU, O'Konek JJ, Janczak KW, Baker JR. Immunomodulation of TH2 biased immunity with mucosal administration of nanoemulsion adjuvant. *Vaccine* 2016;**34**(34):4017-24.

37. Perrie Y, Mohammed AR, Kirby DJ, McNeil SE, Bramwell VW. Vaccine adjuvant systems: enhancing the efficacy of sub-unit protein antigens. *Int J Pharm* 2008;**364**(2):272-80.

38. MacLeod MKL, McKee AS, David A, et al. Vaccine adjuvants aluminum and monophosphoryl lipid a provide distinct signals to generate protective cytotoxic memory CD8 T cells. *Proc Natl Acad Sci U S A* 2011;**108**(19):7914-9.

39. Moyle PM, Toth I. Modern subunit vaccines: development, components, and research opportunities. *ChemMedChem* 2013;**8**(3):360-76.